

Photonic Crystal Cavities in Cubic Polytype Silicon Carbide Films

Marina Radulaski,^{1,*} Thomas M. Babinec,¹ Sonia Buckley,¹ Armand Rundquist,¹ J Provine,² Kassem Alassaad,³ Gabriel Ferro,³ and Jelena Vučković¹

¹E. L. Ginzton Laboratory, Stanford University, Stanford, CA 94305, U.S.A.

²Department of Electrical Engineering, Stanford University, Stanford, CA 94305, U.S.A.

³Laboratoire des Multimateriaux et Interfaces, Université de Lyon, 69622 Villeurbanne Cedex, France

*marina.radulaski@stanford.edu

Abstract: We present the design, fabrication, and characterization of high quality factor ($Q \sim 10^3$) and small mode volume ($V \sim 0.75 (\lambda/n)^3$) planar photonic crystal cavities from cubic (3C) thin films (thickness ~ 200 nm) of silicon carbide (SiC) grown epitaxially on a silicon substrate. We demonstrate cavity resonances across the telecommunications band, with wavelengths from 1.25 – 1.6 μm . Finally, we discuss possible applications in nonlinear optics, optical interconnects, and quantum information science.

OCIS codes: (350.4238) Nanophotonics and photonic crystals ; (160.5293) Photonic band gap materials.

References and links

1. I. Aharonovich, S. Castelletto, D. A. Simpson, C.-H. Su, A. D. Greentree and S. Prawer, “Diamond-based single-photon emitters,” *Rep. Prog. Phys.* **74**, 076501 (2011).
2. E. Togan, Y. Chu, A.S. Trifonov, L. Jiang, J. Maze, L. Childress, M. V. Dutt, A. S. Sorensen, P. Hemmer and A. S. Zibrov, M. Lukin, “Quantum entanglement between an optical photon and a solid-state qubit,” *Nature* **466**, 730-735 (2010).
3. S. Castelletto, B. C. Johnson, N. Stavrias, T. Umeda, and T. Ohshima, “Efficiently engineered room temperature single photons in silicon carbide,” arXiv:1210:5047.
4. K. Rivoire, S. Buckley and J. Vuckovic, “Multiply resonant photonic crystal nanocavities for nonlinear frequency conversion,” *Opt. Express* **19**, 22198-22207 (2011).
5. K. Rivoire, Z. Lin, F. Hatami, W. T. Masselink and J. Vuckovic, “Second harmonic generation in gallium phosphide photonic crystal nanocavities with ultralow continuous wave pump power,” *Opt. Express* **17**, 22609-22615 (2009).
6. S. Buckley, A. Faraon and J. Vuckovic, “Gallium phosphide photonic crystal nanocavities in the visible,” *Appl. Phys. Lett.* **93**, 063106 (2008).
7. A. Gruber, A. Drabenstedt, C. Tietz, L. Fleury, J. Weachtrup and C. von Borczyskowski, “Scanning confocal optical microscopy and magnetic resonance on single defect centers,” *Science* **276**, 2012-2014 (1997).
8. S.-Y. Lee, M. Widmann, T. Rendler, M. Doherty, T. M. Babinec, S. Yang, M. Eyer, P. Siyushev, B. J. M. Hausmann, M. Loncar, Z. Bodrog, A. Gali, N. Manson, H. Fedder, J. Wrachtrup, “Readout and control of a single nuclear spin with a meta-stable electron spin ancilla,” *Nat. Nanotechnol.* **8**, 487-492 (2013).
9. A. M. Zaitsev, *Optical Properties of Diamond* (Springer-Verlag Berlin, 2001).
10. G. Balasubramanian, P. Neumann, D. Twitchen, M. Markham, R. Kolesov, N. Mizuochi, J. Isoya, J. Achard, J. Beck, J. Tissler, V. Jacques, P. R. Hemmer, F. Jelezko and J. Wrachtrup, “Ultralong spin coherence time in isotopically engineered diamond,” *Nature Mater.* **8**, 383-387 (2009).
11. M. Steger, K. Saeedi, M. L. W. Thewalt, J. J. L. Morton, H. Riemann, N. V. Abrosimov, P. Becker and H.-J. Pohl, “Quantum information storage for over 180 s using donor spins in a ^{28}Si semiconductor vacuum,” *Science* **336**, 1280-1283 (2012).
12. A. Faraon, P. E. Barclay, C. Santori, K.-M. C. Fu and R. G. Beausoleil, “Resonant Enhancement of the Zero-Phonon Emission from a Color Centre in a Diamond Cavity,” *Nature Photon.* **5**, 301-305 (2011).
13. A. Faraon, C. Santori, Z. Huang, V. M. Acosta and R. G. Beausoleil, “Coupling of nitrogen-vacancy centers to photonic crystal cavities in monocrystalline diamond,” *Phys. Rev. Lett.* **109**, 033604 (2012).
14. J. T. Choy, B. J. Hausmann, T. M. Babinec, I. Bulu, M. Khan, P. Maletinsky, A. Yacoby and M. Loncar, “Enhanced single-photon emission from a diamond-silver aperture,” *Nature Photon.* **5**, 738-743 (2011).
15. T. M. Babinec, B. J. Hausmann, M. Khan, Y. Zhang, J. R. Maze, P. R. Hemmer and M. Loncar, “A diamond nanowire single photon source,” *Nat. Nanotechnol.* **5**, 195-199 (2010).
16. B. J. M. Hausmann, B. Shields, Q. Quan, P. Maletinsky, M. McCutcheon, J. T. Choy, T. M. Babinec, A. Kubanek, A. Yacoby, M. D. Lukin and M. Loncar, “Integrated diamond networks for quantum nanophotonics,” *Nano Lett.* **12**, 1578-1582 (2012).
17. M. J. Burek, N. P. de Leon, B. J. Shields, B. J. M. Hausmann, Y. Chu, Q. Quan, A. S. Zibrov, H. Park, M. D. Lukin and M. Loncar, “Free-standing mechanical and photonic nanostructures in single-crystal diamond,” *Nano Lett.* **12**, 6084-6089 (2012).
18. G. L. Harris, *Properties of silicon carbide* (INSPEC, 1995).
19. W. Koehl, B. B. Buckley, F. J. Heremans, G. Calusine and D. D. Awschalom, “Room temperature coherent control of defects spin qubits in silicon carbide,” *Nature* **479**, 84-87 (2011).
20. Y. T. Yang, K. L. Ekinci, X. M. H. Huang, L. M. Schiavone, M. L. Roukes, C. A. Zorman and M. Mehregany, “Monocrystalline silicon carbide nanoelectromechanical systems,” *Appl. Phys. Lett.* **78**, 162-164 (2001).

21. M. Mehregany, C. A. Zorman, N. Rajan and C. H. Wu, "Silicon carbide MEMS for harsh environments," *Proceedings of the IEEE* **86**, 1594-1610 (1998).
22. A. L. Falk, B. B. Buckley, G. Calusine, W. F. Koehl, V. V. Dobrovitski, A. Politi, C. A. Zorman, P. X.-L. Feng and D. D. Awschalom, "Polytype control of spin qubits in silicon carbide," *Nat. Commun.* **4**, 1819 (2013).
23. J.-H. Lee, I. Bargatin, J. Park, K. M. Milaninia, L. S. Theogarajan, R. Sinclair and R. T. Howe, "Smart-cut layer transfer of single-crystal SiC using spin-on-glass," *J. Vac. Sci. Technol. B* **30**, 042001 (2012).
24. S. Yamada, B.-S. Song, T. Asano and S. Noda, "Silicon carbide-based photonic crystal nanocavities for ultra-broadband operation from infrared to visible wavelengths," *Applied Physics Letters* **99**, 201102 (2011).
25. B.-S. Song, S. Yamada, T. Asano and S. Noda, "Demonstration of two-dimensional photonic crystals based on silicon carbide," *Optics Express* **19**, 11084-11089 (2011).
26. G. L. Harris, E. W. Jones, M. G. Spencer and K. H. Jackson, "Second harmonic conversion in cubic silicon carbide at 1.06 μm ," *Appl. Phys. Lett.* **59**, 15 (1991).
27. X. Tang, K. G. Irvine, D. Zhang and M. G. Spencer, "Linear electro-optic effect in cubic silicon carbide," *Appl. Phys. Lett.* **59**, 1938-1939 (1991).
28. J. Cardenas, M. Zhang, C. T. Phare, S. Y. Shah, C. B. Poitras and M. Lipson, "High Q SiC microresonators," *Optics Express* **21**, 16882-16887 (2013).
29. X. Lu, J. Y. Lee, P. X.-L. Feng and Q. Lin, "Silicon carbide microdisk resonator," *Optics Letters* **38**, 1304-1306 (2013).
30. M. Eichenfeld, R. Camacho, J. Chan, K. J. Vahala and O. Painter, "A picogram- and nanometre-scale photonic-crystal optomechanical cavity," *Nature* **459**, 550-555 (2009).
31. Y. Akahane, T. Asano and B.-S. Song, "High-Q photonic nanocavity in a two-dimensional photonic crystal," *Nature* **425**, 944-947 (2003).
32. P. B. Deotare, M. W. McCutcheon, I. W. Frank, M. Khan and M. Loncar, "High quality factor photonic crystal nanobeam cavities," *Appl. Phys. Lett.* **94**, 121106 (2009).
33. M. Khan, T. Babinec, M. W. McCutcheon, P. Deotare and M. Loncar, "Fabrication and characterization of high-quality-factor silicon nitride nanobeam cavities," *Opt. Lett.* **36**, 421-423 (2011).
34. Y. Gong and J. Vuckovic, "Photonic crystal cavities in silicon dioxide," *Appl. Phys. Lett.* **96**, 031107 (2010).
35. G. Ferro, T. Chassagne, A. Leycuras, F. Cauwet, and Y. Monteil, *Chemical Vapor Deposition* Vol. 12, Issue 8-9, 483-488 (2006).
36. M. Galli, S. L. Portalupi, M. Belotti, L. C. Andreani, L. OFaolain and T. F. Krauss, "Light scattering and Fano resonances in high-Q photonic crystal nanocavities," *Appl. Phys. Lett.* **94**, 071101 (2009).

Wide band-gap semiconductors have recently emerged as an important material platform for nanophotonics and quantum information science, with applications including room temperature quantum nodes and single photon sources based on diamond and SiC¹⁻³. In nonlinear optics, GaP photonic crystals have been used to perform frequency conversion between near infrared and visible wavelengths⁴⁻⁶, needed for classical and quantum information processing as well as on-chip spectroscopy at arbitrary wavelengths.

Among the aforementioned materials, diamond has been studied most extensively in recent years, because of the combination of its wide optical transparency window, well-known and optically-addressable spin qubits⁷⁻⁹, and advanced materials processing techniques such as isotopic engineering^{10,11}. While recent advances in generating nanophotonic structures in single crystal diamond have been made¹²⁻¹⁷, the inability to grow high-quality single crystal diamond directly on a suitable low-index or sacrificial substrate presents some practical long-term challenge to integration.

On the other hand, silicon carbide¹⁸ has recently been considered as an alternative to diamond with significant material advantages: SiC also possesses optically addressable spin qubits at room temperature¹⁹, but as opposed to diamond, high material purity and electrical control are much easier to achieve as it has been used for many years as a material in electronics and MEMS^{20,21}. Many polytypes of SiC are available, 4H being the most extensively studied for quantum optics¹⁹. However, the cubic polytype (3C) of SiC has a bandgap of 2.4 eV, as well as known impurities akin to NV centers in diamond²². Moreover, optically thin (~ 200 nm) films of 3C-SiC may be grown directly on a silicon substrate¹⁸. This facilitates the fabrication of planar and free-standing devices and eliminates potentially damaging fabrication steps such as ion implantation in a smart-cut process necessary in 4H and 6H polytypes²³⁻²⁵.

Additionally, the 3C polytype possesses a large E/ρ ratio of Young's modulus to mass density^{20,21} for high-frequency applications in opto-mechanics, as well as a strong optical $\chi^{(2)}$ and $\chi^{(3)}$ nonlinearities^{26,27} for applications in frequency conversion.

In this paper we present the design, fabrication, and characterization of photonic crystal cavities in 3C-SiC grown on silicon. This approach differs from recent demonstrations of whispering gallery mode resonators^{28,29} in 3C-SiC in that photonic crystals may possess high quality factors but with dramatically smaller mode volumes. Although we focus on 2D photonic crystal cavities, the approach is directly applicable to 1D nanobeam and crossbeam structures more suitable for opto-mechanics³⁰ and nonlinear optics⁴.

The devices examined in this paper are planar photonic crystal cavities implementing a shifted linear three-hole defect (L3). These cavities (Fig. 1) have their three central holes removed and holes adjacent the cavity center further

displaced outwards by 15% of the lattice constant. The structures are also characterized by a device layer thickness $d \sim 210$ nm, silicon carbide refractive index $n \sim 2.55$, and hole radius $r = 0.3a$. Finite-difference time-domain simulations (FDTD) indicate that these structures possess theoretical mode volume values $V \sim 0.75 (\lambda/n)^3$ and cavity quality factors $Q \sim 2,000$. Lowering the radius of the holes nearest to the cavity can theoretically improve quality factor to $Q \sim 5,000$, but it also imposes fabrication challenge due to the reduced feature size. In the future, we may design higher- Q cavities and overcome the low refractive index of 3C silicon carbide by implementing either 2D heterostructure³¹ or 1D nanobeam³²⁻³⁴ designs.

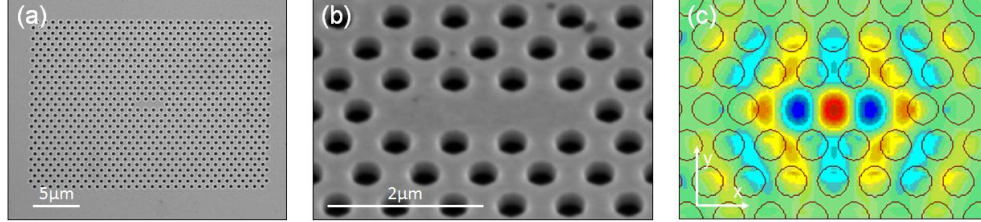


Fig. 1. SEM of fabricated 3C-SiC shifted L3 cavity from (a) orthogonal incidence and (b) 40-degree tilt (c) FDTD simulation of the dominant (E_y) electric field component of the fundamental mode, with the outlines of the holes indicated.

The fabrication process flow to realize the 3C-SiC photonic crystal cavities is presented in Fig. 2. The starting material consists of a 3C-SiC layer grown epitaxially on a 35 mm diameter Si substrate using a standard two-step chemical vapor deposition (CVD) process³⁵. The film thickness $d \sim 210$ nm and refractive index ($n \sim 2.55$ at 1300 – 1500 nm) were confirmed using a Woollam spectroscopic ellipsometer before proceeding to subsequent masking and etching steps. A SiO_2 hard mask was then deposited using a low-pressure CVD furnace followed by SiO_2 thinning in a 2% HF solution to the target thickness of 200-250 nm. Next, a second mask layer (Fig. 2a) of ~ 400 nm of electron beam lithography resist (ZEP 520a) was spun. Photonic crystal cavities were then patterned at the base-dose range 250 – 400 $\mu\text{C}/\text{cm}^2$ using a 100 keV electron beam lithography tool (JEOL JBX 6300) and then developed using standard recipes (Fig. 2b-c). The initial pattern transfer from resist into SiO_2 (Fig. 2d) was performed using CF_4 , CHF_3 , and Ar chemistry in a plasma etching system (Advanced Materials, p5000). Etch tests on bare (un-patterned) chips indicated that the selectivity of this etch was approximately 1:1 (SiO_2 to ZEP). Residual electron beam resist was then completely removed in Microposit remover 1165 (Fig. 2e), and a second pattern transfer from SiO_2 into SiC using HBr and Cl_2 chemistry (Fig. 2f) was performed in the same system. Etch tests on bare chips indicated that the selectivity was approximately 2:1 (SiC to SiO_2). Next, undercutting of the SiC device layer was achieved by isotropic etching of the underlying Si (Fig. 2g) with a XeF_2 vapor phase etcher (Xactix e-1). Finally, the remaining SiO_2 hard mask layer was removed in 2% HF solution (Fig. 2h).

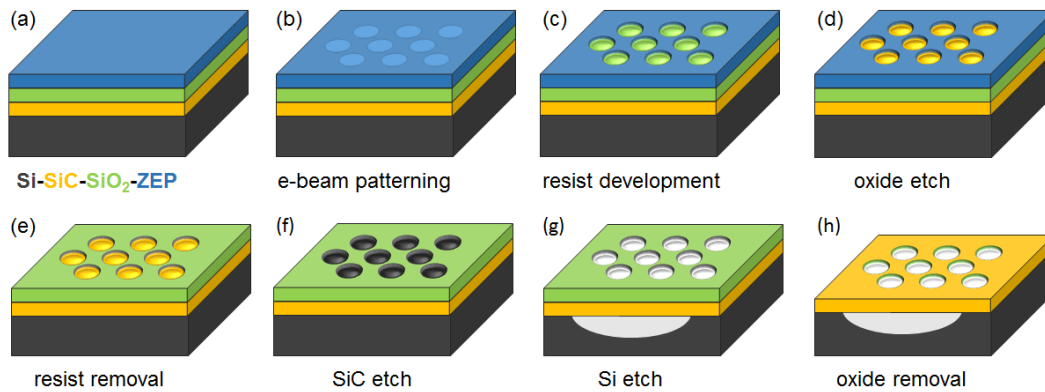


Fig. 2. The process flow to generate suspended photonic crystal structures in 3C-SiC films.

The fabricated 3C-SiC photonic crystal cavities were characterized using a cross-polarization measurement technique with apparatus presented in Fig. 3a. In this experiment, a halogen lamp (Ocean Optics) provided broadband excitation of the L3 cavity resonances in the wavelength region 1250 – 1600 nm and a high numerical aperture ($NA = 0.5$) objective lens was used to optically address the cavity with high efficiency. Incoming light was first polarized vertically and reflected off the polarizing beam splitter (PBS) towards the sample, with orthogonally polarized cavities

oriented at +45 degrees. A half wave plate (HWP), positioned between the PBS and the objective, controlled both coupling to the cavity as well as transmission through the PBS towards a liquid nitrogen-cooled InGaAs spectrometer (Princeton Instruments) to monitor the resonance spectra.

High signal/noise ratio of maximum cavity coupled-light signal to uncoupled background light is achieved when the fast axis of the HWP rotates and aligns the polarization of the incoming beam orthogonal to the cavity (-45 degrees). Fig. 3b shows one such spectrum of the fundamental mode of a representative 3C-SiC cavity at 1530 nm with quality factor of 800, obtained from a fit to Fano-resonance³⁶. Deviations from the design (simulation predicted $Q \sim 1500$ in the case of the presented resonance) can be attributed to fabrication imperfections and/or the crystalline defects present in the 3C-SiC material due to the lattice mismatch. Moreover, rotating the HWP modifies the cavity coupled light at the output so that the peak intensity of the cavity resonance has $\sin(4\theta)$ dependence. The polarization-dependent signal presented in Fig. 3c shows good agreement with this theory.

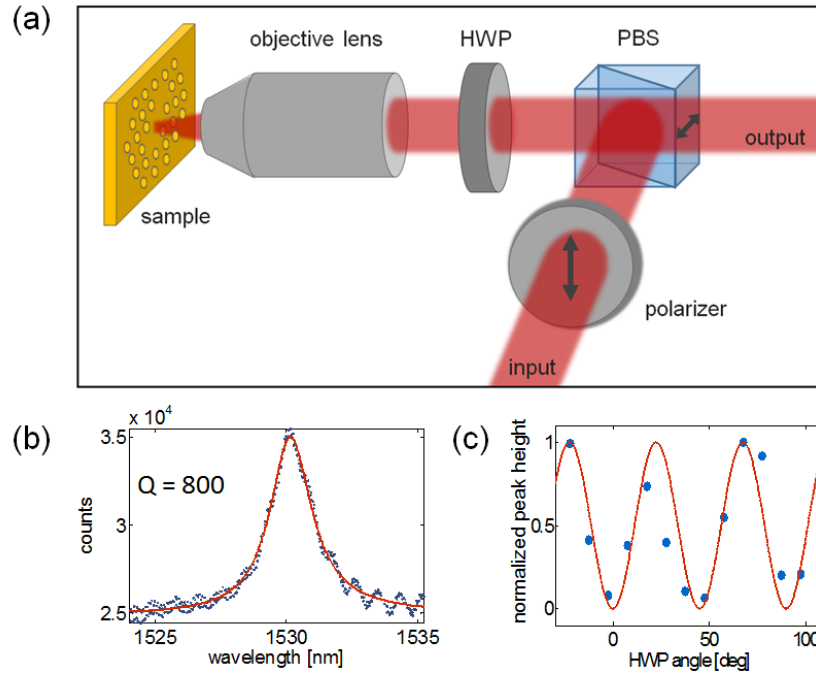


Fig. 3. (a) Cross-polarized reflectivity setup scheme, (b) characterized fundamental mode resonance at telecommunications wavelength, blue dots represent data points, red line shows fit to a Fano-resonance with quality factor of 800, (c) resonance intensity dependence on polarization angle of incoming light, blue dots represent data points, red line shows fit to $\sin(4\theta)$, where θ is half-wave plate rotation angle.

For most applications, it is necessary to be able to controllably target resonance wavelengths of high-Q cavities both over a large range and to specific wavelengths of interest (e.g. lines of optical emitters). In order to generate cavities that are tunable across the telecommunications band, we therefore varied the lattice constant a of the L3 cavities in the range 500 – 700 nm. We again monitored the resonant wavelength and quality factor of the fundamental modes of these structures via the cross-polarized reflectivity technique. The results of this experiment, which are presented in Fig. 4, show that resonances of L3 cavities of $Q \sim 10^3$ may be achieved across wavelengths 1250 – 1600 nm.

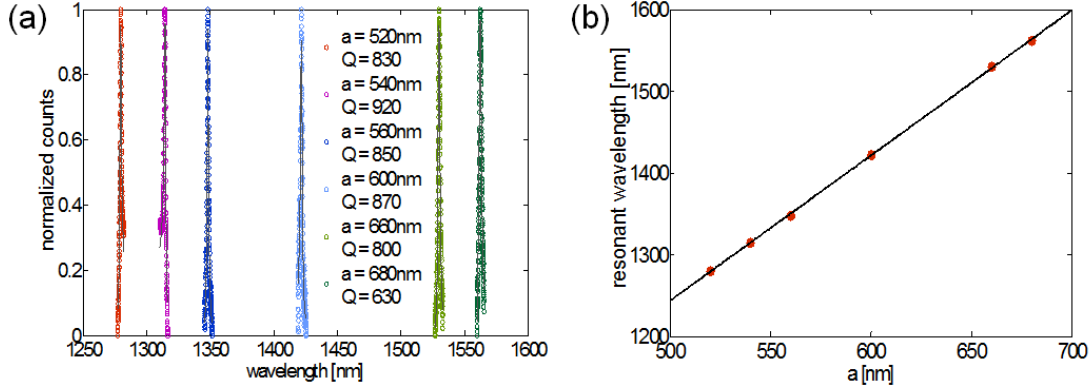


Fig. 4. (a) Fundamental mode resonance scaling with lattice constant a , shown with Fano-resonance fit with quality factors in range 630 to 920; all cavities are shifted L3 cavities made in 207 nm thick slab of 3C-SiC. (b) Experimentally measured linear dependence of resonant wavelength on lattice constant.

In conclusion, we have demonstrated photonic crystal cavities in the 3C-SiC thin films operating at telecommunications wavelengths. The fabrication routine is robust and should allow for a diverse set of devices such as nanobeam photonic crystal cavities and photonic crystal waveguides at diverse wavelengths including the near infrared and visible. The demonstrated scalable fabrication process would enable wider use of 3C-SiC nanophotonic classical and quantum information processing.

Acknowledgements

This work was supported by the Presidential Early Career Award for Scientists and Engineers (PECASE) from the Office of Naval Research and National Science Foundation (Grant ECCS- 10 25811), M.R. and S.B. were also supported by the Stanford Graduate Fellowships and National Science Graduate Fellowship. TMB was supported by the Nanoscale and Quantum Science and Engineering Postdoctoral Fellowship. We thank Helmut Fedder, Jörg Wrachtrup, and Phillip Hemmer for helpful discussions. This work was performed in part at the Stanford Nanofabrication Facility of NNIN supported by the National Science Foundation under Grant No. ECS-9731293.